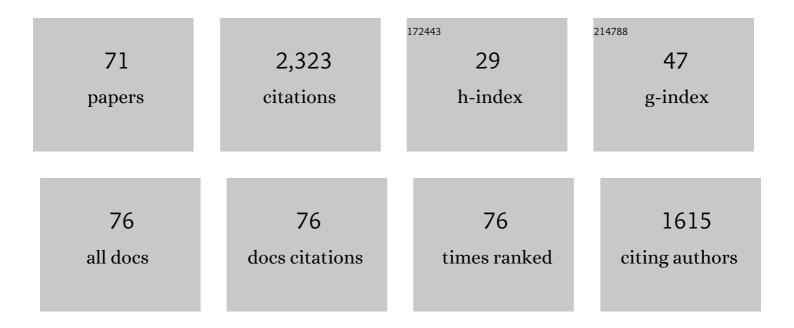
Oliver Ritter

List of Publications by Year in descending order

Source: https://exaly.com/author-pdf/3462230/publications.pdf Version: 2024-02-01



#	Article	IF	CITATIONS
1	Three-dimensional magnetotelluric imaging of the Mérida Andes, Venezuela. Journal of South American Earth Sciences, 2022, 114, 103711.	1.4	0
2	Magnetotelluric imaging of the Mérida Andes and surrounding areas in Venezuela. Geophysical Journal International, 2020, 222, 1570-1589.	2.4	4
3	Neoproterozoic amalgamation and Phanerozoic reactivation of Central/Western Hoggar (Southern) Tj ETQq1 139, 101764.	1 0.784314 1.6	rgBT /Overlo 10
4	Repeatability of land-based controlled-source electromagnetic measurements in industrialized areas and including vertical electric fields. Geophysical Journal International, 2019, 218, 1552-1571.	2.4	9
5	Elongated horizontal and vertical receivers in threeâ€dimensional electromagnetic modelling and inversion. Geophysical Prospecting, 2019, 67, 2227-2244.	1.9	0
6	Fluid Distribution in the Central Andes Subduction Zone Imaged With Magnetotellurics. Journal of Geophysical Research: Solid Earth, 2019, 124, 4017-4034.	3.4	35
7	Borehole Controlled–Source Electromagnetics for Hydrocarbon–Saturation Monitoring in the Bockstedt Oil Field, Onshore Northwest Germany. SPE Reservoir Evaluation and Engineering, 2018, 21, 364-372.	1.8	3
8	A land-based controlled-source electromagnetic method for oil field exploration: An example from the Schoonebeek oil field. Geophysics, 2018, 83, WB1-WB17.	2.6	14
9	Steel-cased wells in 3-D controlled source EM modelling. Geophysical Journal International, 2017, 209, 813-826.	2.4	35
10	Time-lapse CSEM inversion using focusing regularization techniques for reservoir monitoring. , 2017, , \cdot		1
11	Crustal metamorphic fluid flux beneath the Dead Sea Basin: constraints from 2-D and 3-D magnetotelluric modelling. Geophysical Journal International, 2016, 207, 1609-1629.	2.4	22
12	The electrical conductivity of Posidonia black shales — from magnetotelluric exploration to rock samples. Geophysical Prospecting, 2016, 64, 469-488.	1.9	11
13	Timelapse Borehole CSEM for HC-Saturation Monitoring in the Bockstedt Oilfield Onshore NW Germany. , 2016, , .		5
14	3-D magnetotelluric image of offshore magmatism at the Walvis Ridge and rift basin. Tectonophysics, 2016, 683, 98-108.	2.2	15
15	Electrical resistivity image of the South Atlantic continental margin derived from onshore and offshore magnetotelluric data. Geophysical Research Letters, 2016, 43, 154-160.	4.0	10
16	Source effects in mid-latitude geomagnetic transfer functions. Geophysical Journal International, 2016, 204, 606-630.	2.4	14
17	Borehole Controlled Source Electromagnetic (CSEM) Surveying for Monitoring HC-Saturation in the Bockstedt Oilfield (NW Germany). , 2015, , .		2
18	Controlledâ€source electromagnetic monitoring of reservoir oil saturation using a novel boreholeâ€soaî€surface configuration. Geophysical Prospecting, 2015, 63, 1468-1490.	1.9	62

OLIVER RITTER

#	Article	IF	CITATIONS
19	Joint 3D inversion of multiple electromagnetic datasets. Geophysical Prospecting, 2015, 63, 1450-1467.	1.9	21
20	3-D joint inversion of the magnetotelluric phase tensor and vertical magnetic transfer functions. Geophysical Journal International, 2015, 203, 1128-1148.	2.4	39
21	CSEM Monitoring of Reservoir Oil-saturation Using a Novel Borehole-to-surface Configuration. , 2015, , .		6
22	CSEM for monitoring reservoir oil-saturation using a borehole-to-surface set-up. , 2015, , .		0
23	Recent Developments for Land-based Controlled-source Electromagnetic Surveying. , 2014, , .		4
24	3D inversion and resolution analysis of land-based CSEM data from the Ketzin CO2 storage formation. Geophysics, 2014, 79, E101-E114.	2.6	73
25	Resistivity structure underneath the Pamir and Southern Tian Shan. Geophysical Journal International, 2014, 198, 564-579.	2.4	47
26	Electromagnetic Monitoring of the Propagation of an Injected Polymer for Enhanced Oil Recovery in Northern Germany. , 2014, , .		8
27	Three-Dimensional Multi-Scale and Multi-Method Inversion to Determine the Electrical Conductivity Distribution of the Subsurface (Multi-EM). Advanced Technologies in Earth Sciences, 2014, , 83-93.	0.9	0
28	Implementing novel schemes for inversion of 3D EM data in ModEM, the OSU modular EM inversion system. , 2014, , .		0
29	Three-dimensional parallel distributed inversion of CSEM data using a direct forward solver. Geophysical Journal International, 2013, 193, 1432-1446.	2.4	128
30	Three-dimensional magnetotelluric inversion in practice—the electrical conductivity structure of the San Andreas Fault in Central California. Geophysical Journal International, 2013, 195, 130-147.	2.4	103
31	Robust processing of noisy land-based controlled-source electromagnetic data. Geophysics, 2013, 78, E237-E247.	2.6	54
32	A magnetotelluric transect across the Dead Sea Basin: electrical properties of geological and hydrological units of the upper crust. Geophysical Journal International, 2013, 193, 1415-1431.	2.4	14
33	Pseudoâ€remote reference processing of magnetotelluric data: a fast and efficient data acquisition scheme for local arrays. Geophysical Prospecting, 2013, 61, 300-316.	1.9	13
34	Direct penetration of the interplanetary electric field to low geomagnetic latitudes and its effect on magnetotelluric sounding. Journal of Geophysical Research, 2012, 117, .	3.3	9
35	Nearâ€surface properties of an active fault derived by joint interpretation of different geophysical methods ―the Arava/Araba Fault in the Middle East. Near Surface Geophysics, 2012, 10, 381-390.	1.2	3
36	Magnetotelluric image linked to surface geology across the Cape Fold Belt, South Africa. Terra Nova, 2012, 24, 207-212.	2.1	12

OLIVER RITTER

#	Article	IF	CITATIONS
37	Magnetotelluric Studies at the San Andreas Fault Zone: Implications for the Role of Fluids. Surveys in Geophysics, 2012, 33, 65-105.	4.6	73
38	Shallow lithological structure across the Dead Sea Transform derived from geophysical experiments. Geochemistry, Geophysics, Geosystems, 2011, 12, n/a-n/a.	2.5	6
39	Correlation between deep fluids, tremor and creep along the central San Andreas fault. Nature, 2011, 480, 87-90.	27.8	170
40	2.5D controlled-source EM modeling with general 3D source geometries. Geophysics, 2011, 76, F387-F393.	2.6	17
41	Strategies for land-based controlled-source electromagnetic surveying in high-noise regions. The Leading Edge, 2011, 30, 1174-1181.	0.7	27
42	Exploring the Groß Schönebeck (Germany) geothermal site using a statistical joint interpretation of magnetotelluric and seismic tomography models. Geothermics, 2010, 39, 35-45.	3.4	47
43	A target-oriented magnetotelluric inversion approach for characterizing the low enthalpy Groß Schönebeck geothermal reservoir. Geophysical Journal International, 2010, 183, 1199-1215.	2.4	25
44	Imaging of CO2 storage sites, geothermal reservoirs, and gas shales using controlled-source magnetotellurics: Modeling studies. Chemie Der Erde, 2010, 70, 63-75.	2.0	42
45	Simple models for the Beattie Magnetic Anomaly in South Africa. Tectonophysics, 2009, 478, 111-118.	2.2	13
46	Anatomy of the Dead Sea Transform from lithospheric to microscopic scale. Reviews of Geophysics, 2009, 47, .	23.0	56
47	Mode separation of magnetotelluric responses in three-dimensional environments. Geophysical Journal International, 2008, 172, 67-86.	2.4	49
48	A deep crustal fluid channel into the San Andreas Fault system near Parkfield, California. Geophysical Journal International, 2008, 173, 718-732.	2.4	77
49	Geophysical Characterization of the Gross Schoenebeck Low Enthalpy Geothermal Reservoir. , 2008, , .		1
50	Comparison of electrical conductivity structures and 2D magnetic modelling along two profiles crossing the Beattie Magnetic Anomaly, South Africa. South African Journal of Geology, 2007, 110, 449-464.	1.2	29
51	The Whitehill Formation a high conductivity marker horizon in the Karoo Basin. South African Journal of Geology, 2007, 110, 465-476.	1.2	32
52	Magnetotelluric measurements across the Beattie magnetic anomaly and the Southern Cape Conductive Belt, South Africa. Journal of Geophysical Research, 2007, 112, .	3.3	36
53	Lithology-derived structure classification from the joint interpretation of magnetotelluric and seismic models. Geophysical Journal International, 2007, 170, 737-748.	2.4	75

OLIVER RITTER

#	Article	IF	CITATIONS
55	Em, Regional Studies. , 2007, , 242-245.		0
56	Effective noise separation for magnetotelluric single site data processing using a frequency domain selection scheme. Geophysical Journal International, 2005, 161, 635-652.	2.4	114
57	Electrical conductivity images of active and fossil fault zones. Geological Society Special Publication, 2005, 245, 165-186.	1.3	59
58	Characterizing a large shear-zone with seismic and magnetotelluric methods: The case of the Dead Sea Transform. Geophysical Research Letters, 2005, 32, .	4.0	29
59	The crustal structure of the Dead Sea Transform. Geophysical Journal International, 2004, 156, 655-681.	2.4	107
60	Correlation of electrical conductivity and structural damage at a major strike-slip fault in northern Chile. Journal of Geophysical Research, 2004, 109, .	3.3	35
61	A high-resolution magnetotelluric survey of the Iapetus Suture Zone in southwest Scotland. Geophysical Journal International, 2003, 153, 548-568.	2.4	26
62	lmages of the magnetotelluric apparent resistivity tensor. Geophysical Journal International, 2003, 155, 456-468.	2.4	23
63	Geophysical images of the Dead Sea Transform in Jordan reveal an impermeable barrier for fluid flow. Geophysical Research Letters, 2003, 30, .	4.0	53
64	A magnetotelluric study of the Damara Belt in Namibia. Physics of the Earth and Planetary Interiors, 2003, 138, 71-90.	1.9	57
65	A magnetotelluric study of the Damara Belt in Namibia. Physics of the Earth and Planetary Interiors, 2003, 138, 91-112.	1.9	57
66	Magnetotelluric and geomagnetic modelling reveals zones of very high electrical conductivity in the upper crust of Central Java. Physics of the Earth and Planetary Interiors, 2001, 124, 131-151.	1.9	45
67	Multinational geoscientific research effort kicks off in the Middle East. Eos, 2000, 81, 609-617.	0.1	13
68	Very high electrical conductivity beneath the Munchberg Gneiss area in Southern Germany: implications for horizontal transport along shear planes. Geophysical Journal International, 1999, 139, 161-170.	2.4	15
69	New equipment and processing for magnetotelluric remote reference observations. Geophysical Journal International, 1998, 132, 535-548.	2.4	110
70	A magnetotelluric profile across Central Java, Indonesia. Geophysical Research Letters, 1998, 25, 4265-4268.	4.0	11
71	GIPP: Geophysical Instrument Pool Potsdam. Journal of Large-scale Research Facilities JLSRF, 0, 2, A64.	0.0	5